

ALCHEMI: Results from the ALMA Comprehensive High-resolution Extragalactic Molecular Inventory of NGC 253

Jeffrey G. Mangum^{1,*}, Serena Viti^{2,3,**}, and The ALCHEMI Collaboration^a

¹National Radio Astronomy Observatory, 520 Edgemont Road, Charlottesville, VA 22903-2475, USA

²Leiden Observatory, Leiden University, PO Box 9513, 2300 RA Leiden, The Netherlands

³Department of Physics and Astronomy, University College London, Gower Street, London WC1E 6BT, UK

Abstract. The star formation process in galaxies drives their evolution. The physical conditions which drive the star formation process in galaxies are studied using measurements of atomic and molecular species found in the dense gas from which stars form in galaxies. Molecular emission measurements at millimeter/submillimeter wavelengths have revealed the molecular complexity of the star formation regions in galaxies. In a recent study of the nearby starburst galaxy NGC 253 using the Atacama Large Millimeter/submillimeter Array (ALMA), the ALMA Comprehensive High-resolution Extragalactic Molecular Inventory (ALCHEMI) large program imaged the continuum and spectral line emission from the central molecular zone (CMZ) of this starburst galaxy. In this article we summarize the current results derived from the ALCHEMI large program. Many of these studies have focused on clarifying the state of dense gas heating processes in the NGC 253 CMZ.

1 Introduction

The study of the star formation process in galaxies requires a wide array of diverse measurements at all wavelengths. Central to the early phases of the star formation process are measurements of the atomic and molecular spectral line and continuum emission toward those regions in galaxies which are, or will in the near future, form stars [10]. Starburst galaxies sit at the extreme end of the spectrum of star formation activities in galaxies due to their extreme star-forming environments as compared to the Milky Way. Observing starburst galaxies allows us to study how stars form in regions with high densities and temperatures. The proper characterization of the physical conditions in extragalactic star-forming regions requires high spatial resolution and sensitivity which will allow for the study of structures on giant molecular cloud (GMC) scales at millimeter/submillimeter wavelengths. Molecular spectral line emission in galaxies is driven by processes associated with star formation (mechanical heating in the form of shocks and turbulence from supernova explosions, radiative heating from massive stars, ionization by cosmic rays from supernova remnants, etc.) that have competing effects on the interstellar medium (ISM). Determining the influence of each of these physical processes on extragalactic star-forming regions is crucial to our understanding of the chemical and physical processes that guide star formation in starburst environments.

*e-mail: jeff.mangum@nrao.edu

**e-mail: viti@strw.leidenuniv.nl

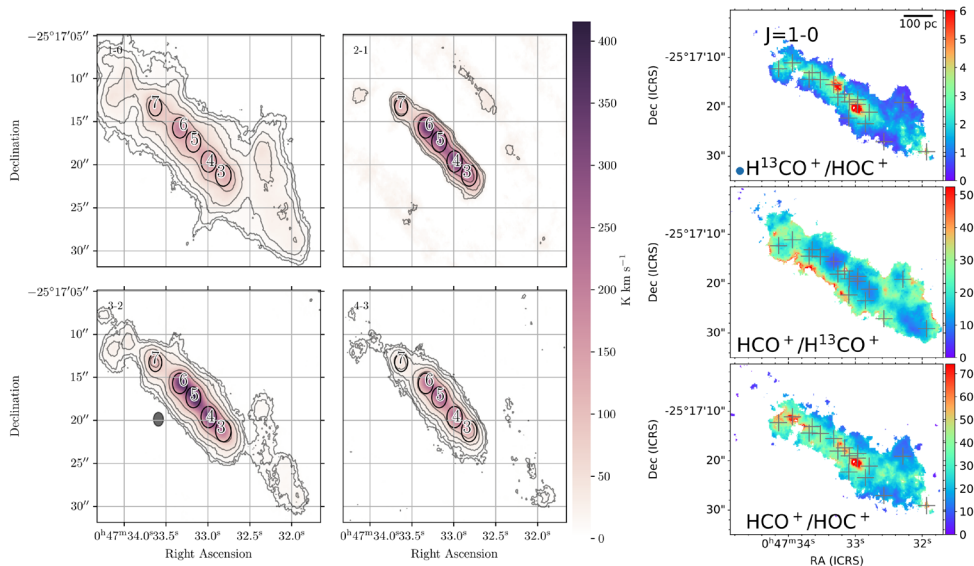


Figure 2. Left: Primary beam-correlated emission maps of C_2H in NGC 253 (from [7]). The beam size for all panels is $1.6''$ and is shown in the bottom left panel. Contours at the 3, 5, 10, 20 and 50σ level are drawn in black. The noise levels in order of increasing N are 1.4, 8.5, 2.0 and 1.6 K km/s . Each ellipse shows the position and size of the Gaussian fits to the four individual clumps described in [7]. The numbers indicate the position of the GMCs. Right: Ratios of velocity-integrated intensity images of the HCO^+ , HOC^+ , and $H^{13}CO^+$ $J=1-0$ emission toward NGC 253 (from [4]). GMC positions indicated by + symbols.

3 Heating Processes Driving Star Formation in NGC 253

Several studies of the physical and chemical conditions in the NGC 253 CMZ have investigated the processes which heat the dense gas in the primary source of the starburst in this galaxy. C_2H [Figure 2; 7], H_3O^+/SO [Figure 3; 6], and HCN/HNC [2] emission characteristics have been used to constrain chemical (UCLCHEM; [5]) and physical (SpectralRadex¹) models of the dense gas. A similar analysis of the HCO^+/HOC^+ emission [4] provided additional information on the CMZ physical conditions. All of these studies found that $T_K > 50 \text{ K}$ and $n(H_2) > 10^5 \text{ cm}^{-3}$, with the high kinetic temperatures driven by cosmic ray ionization rates (CRIRs) 10^{-15} to 10^{-12} s^{-1} , more than 100 times larger than the average CRIR found in the Milky Way. Furthermore, the low measured HCN/HNC abundance ratios are inconsistent with the existence of substantial mechanical heating in the NGC 253 CMZ.

References

- [1] Barrientos, A., Holdship, J. Solar, M., *et al.*, *Experimental Astronomy*, **52**, 157 (2021)
- [2] Behrens, E., Mangum, J. G., Holdship, J., *et al.*, *ApJ*, **submitted** (2022)
- [3] Haasler, D., Rivilla, V. M., Martín, S., *et al.*, *A&A*, **659**, A158 (2022)
- [4] Harada, N., Martín, S., Mangum, J. G., *et al.*, *ApJ*, **923**, A24 (2021)
- [5] Holdship, J., Viti, S., Jiméenez-Serra, I., *et al.*, *AJ*, **154**, 38 (2017)

¹<https://spectralradex.readthedocs.io/>

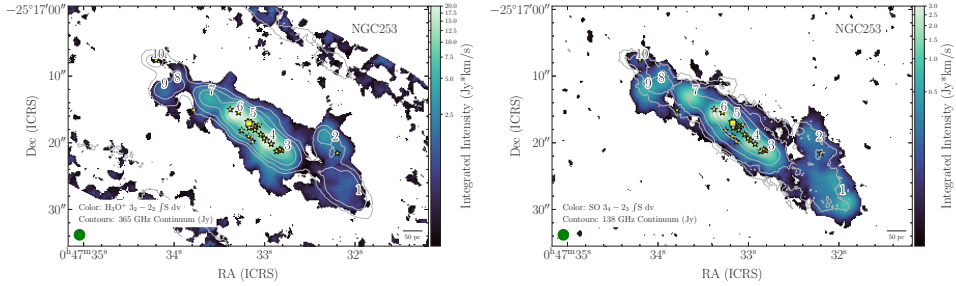


Figure 3. H_3O^+ $3_2 - 2_1$ (left) and SO $3_4 - 2_3$ (right) integrated intensity (moment 0) images toward NGC 253. The green ellipse and black scale bar in the lower-left and lower-right corners show the final imaged beam size (1.6 arcsec) and physical scale, respectively. Black numbers indicate the locations of the GMCs. Star shaped markers locate the positions of the 2 cm radio continuum emission peaks [13], with a square indicating the position of the strongest radio continuum peak. The lower integrated intensity limit for each transition is set to 3σ in the integrated intensity. Overlain in contours is the associated continuum emission distribution for each transition. From [6].

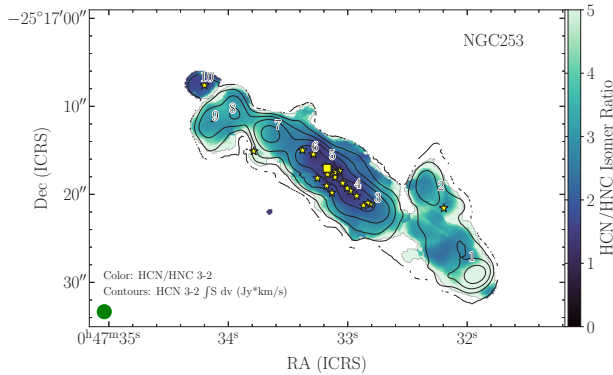


Figure 4. HCN/HNC $J=3 - 2$ integrated intensity ratio (from [2]). Symbols and contours same as Figure 3.

- [6] Holdship, J., Mangum, J. G., Viti, S., *et al.*, *ApJ*, **in press** (2022)
- [7] Holdship, J., Viti, S., Martín, S., *et al.*, *A&A*, **654**, A55 (2021)
- [8] Humire, P. K., Henkel, C., Hernández-Gómez, A., *et al.*, *A&A*, **in press** (2022)
- [9] Leroy, A. K., Bolatto, A. D., Ostriker, E. C., *et al.*, *ApJ*, **801**, 25 (2015)
- [10] Leroy, A. K., Bolatto, A. D., Ostriker, E. C., *et al.*, *ApJ*, **869**, 126 (2018)
- [11] Martín, S., Mangum, J. G., Harada, N., *et al.*, *A&A*, **656**, A46 (2021)
- [12] Spilker, J. S., Marrone, D. P., Aguirre, J. E., *et al.*, *ApJ*, **785**, 149 (2014)
- [13] Ulvestad, J. S., & Antonucci, R. R. J., *ApJ*, 488, 621 (1997)

^aSergio Martín (ESO); Nanase Harada (NAOJ); Rebeca Aladro (MPIfR); Erica Behrens (Department of Astronomy, University of Virginia); Laura Colzi (INAF); Kimberly L. Emig (NRAO); Santiago García-Burillo (OAN-IGN); Christian Henkel (MPIfR); Rubén Herrero-Illana (ESO); Jonathan Holdship (Leiden Observatory/UCL); Ko-Yun Huang (Leiden Observatory); P. K. Humire (MPIfR); Leslie K. Hunt (INAF); Takuma Izumi (NAOJ); Kotaro Kohno (University of Tokyo); David S. Meier (NMT); Sebastien Muller (Chalmers University of Technology); Kouichiro Nakanishi (NAOJ); Víctor M. Rivilla (CSIC-INTA); Kazushi Sakamoto (ASIAA); Kunihiko Tanaka (Keio University); Paul P. van der Werf (Leiden Observatory); Yuki Yoshimura (University of Tokyo)